

Magnetic properties of Ni-Mo single crystal alloys : theory and experiment

Subhradip Ghosh † and Nityananda Das

S.N. Bose National Centre for Basic Sciences, JD Block, Sector 3, Salt Lake City, Calcutta 700091, India.

Abhijit Mookerjee §

Department of Physics, Indian Institute of Technology, Kanpur 208016, India

Abstract. The magnetization of $\text{Ni}_{1-x}\text{Mo}_x$ single crystals with $x=4,6,8$ and 10 % by weight have been measured at 4.2K using a vibrating sample magnetometer and a Superconducting Quantum Interference Device (SQID). The magnetization of the alloy at these low concentrations and at 0K have been theoretically determined by using the tight-binding linearized muffin-tin orbital method coupled with augmented space recursion. The theoretical data are compared with the experiment.

PACS numbers: 71.20,71.20c

1. Introduction

The equilibrium phase diagram of the $\text{Ni}_{1-x}\text{Mo}_x$ system exhibits a continuous face centred cubic disordered solid solution in the range $0 < x \leq 0.12$. The alloy shows a series of ordered phases at higher concentrations [1]. Das *et al* [2] have studied the phase diagram at the higher concentration range using the local density approximation (LDA) based tight-binding linearized muffin-tin approximation (TB-LMTO) method proposed by Andersen *et al* [3]. To our knowledge a similar study of the disordered regime has not been carried out in detail. In this communication we shall report such a study using the same TB-LMTO methodology as before but combining this with the augmented space recursion proposed by one of us [4] to take care of the disorder configuration averaging. We shall evaluate the local magnetization as a function of the Mo concentration. Simultaneously, we shall measure the magnetization of four

† Corresponding author. E-mail : subhra@boson.bose.res.in

§ On sabbatical leave from : S.N. Bose National Centre for Basic Sciences, India

alloy systems in this disordered alloy regime ($x=0.04, 0.06, 0.08$ and 0.1). Side by side we shall compare our results with experimental work on the magnetization and Curie temperatures of single crystals of NiMo [5].

2. Theoretical Details

The TB-LMTO has been described in great detail earlier [6]. We shall refer the reader to the referenced monograph for technical details.

Description of magnetic phases within the local spin density approximation (LSDA) involves the study of the evolution of local magnetic moments in the vicinity of ion cores because of the distribution of the valence electron charge. Each lattice site in the face centred cubic structure is occupied by an ion core : in our case randomly by either Ni or Mo. We shall associate a cell or a sphere with each ion core and assume that the charge contained in the sphere belongs to that ion core alone. Ideally such cells or spheres should not overlap. In the traditional Kohn-Korringa-Rostocker (KKR) method this is certainly so. However, in the atomic sphere approximation (ASA) which we shall use in our TB-LMTO version, this division of space is to a certain extent arbitrary. Within these cells the valence electrons carrying spin σ sees a binary random spin-dependent potential $V_\sigma^\lambda(\underline{r})$, where $\lambda = \text{Ni or Mo}$ and $\sigma = \uparrow$ or \downarrow .

The charge density within the cells can be obtained from solving the Schrödinger equation within the LSDA. The charge density over the solid can be written as :

$$\rho_\sigma(\underline{r}) = -(1/\pi)\mathfrak{Im} \sum_L \int_{-\infty}^{E_F} \left[x \ll G_{LL}^{Mo,\sigma}(\underline{r}, \underline{r}, E) \gg + (1-x) \ll G_{LL}^{Ni,\sigma}(\underline{r}, \underline{r}, E) \gg \right] dE$$

where,

$\ll G_{LL}^{Mo,\sigma}(\underline{r}, \underline{r}, E) \gg$ and $\ll G_{LL}^{Ni,\sigma}(\underline{r}, \underline{r}, E) \gg$ are partially averaged Green functions with the site \underline{r} occupied by a Mo or Ni ion core potential corresponding to spin σ . The Mo sites are almost spin independent (except for a very small induced moment) and do not appreciably contribute to local moment densities.

The averaging is done over configurations of the random alloy. A powerful technique of carrying out this averaging is the augmented space recursion [7]. The method allows us to go well beyond the traditional single site coherent potential approximations and has been applied successfully to a wide variety of systems [8, 9]. The convergence of the ASR has been established recently [11], so that any approximation we impose on the recursion is controlled by tolerance limits preset by us.

For the random ferromagnetic phase we proceed as follows : we consider all cells to be identical in that they all carry identical average charge densities. We shall borrow the notation of Andersen *et al* [3] to write functions like $\tilde{f}(\underline{r}_R)$ which are equal to $f(\underline{r})$ when \underline{r} lies in the atomic sphere labelled by R and is zero outside. The ferromagnetic charge densities are defined as :

$$\begin{aligned}\rho_1(\underline{r}) &= \sum_R \tilde{\rho}_\uparrow(\underline{r}_R) \\ \rho_2(\underline{r}) &= \sum_R \tilde{\rho}_\downarrow(\underline{r}_R)\end{aligned}$$

The magnetic moment per cell (atom) is then defined by :

$$\begin{aligned}m &= (1/N) \int d^3\underline{r} [\rho_1(\underline{r}) - \rho_2(\underline{r})] \\ &= (1/N) \sum_R \int_{r \leq S} d^3\underline{r} [\tilde{\rho}_\uparrow(r_R) - \tilde{\rho}_\downarrow(r_R)] \\ &= (1/N) \sum_R \int_{r \leq S} d^3\underline{r} m_R(r_R)\end{aligned}$$

Since all cells are identical, the above calculation need be done only in one typical cell. Within the TB-LMTO-ASA the cells are replaced by inflated atomic spheres and the remaining interstitial is neglected. The problem is then one of a binary alloy with an almost non-magnetic charge density due to the Mo ion cores and a magnetic one due to the Ni ones.

For the calculation of the component projected averaged density of states of the ferromagnetic phase we have used a real space cluster of 400 atoms and an augmented space shell upto the sixth nearest neighbour from the starting state. Eight pairs of recursion coefficients were determined exactly and the continued fraction terminated by the analytic terminator due to Luchini and Nex [10]. In a recent paper Ghosh *et al* [11] have shown the convergence of the related integrated quantities, like the Fermi energy, the band energy, the magnetic moments and the charge densities, within the augmented space recursion. The convergence tests suggested by the authors were carried out to prescribed accuracies. We have reduced the computational burden of the recursion in the full augmented space by using the local symmetries of the augmented space to reduce the effective rank of the invariant subspace in which the recursion is confined [7] and using the seed recursion methodology [12] with fifteen energy seed points uniformly across the spectrum. Both the reduction techniques have been described in detail in the referenced papers and the readers are referred to them for details. It is important to emphasize this point, since there has been erroneous statements made earlier that although the augmented space recursion method is attractive mathematically, it was not feasible for application as a computational technique is realistic alloys. Further, it has been shown [7] that augmented space recursion with an analytic terminator *always* produces herglotz results, whether we use the homogeneous disorder model as in this paper or the version including short-ranged order [8] or local lattice distortions [9].

We have chosen the Wigner-Seitz radii of the two constituent atoms Mo and Ni in such a way that the average volume occupied by the atoms is conserved. Within this constraint we have varied the radii so that the final configuration has neutral spheres. This eliminates the necessity to include the averaged Madelung Energy part in the total energy of the alloy. The definition and computation of the Madelung Energy in a random alloy had faced controversy in recent literature and to this date no satisfactory resolution of the problem exists. Simultaneously we have made sure that the sphere overlap remains within the 15% limit prescribed by Andersen.

The calculations have been made self-consistent in the LSDA sense, that is, at each stage the averaged charge densities are calculated from the augmented space recursion and the new potential is generated by the usual LSDA techniques. This self-consistency cycle was converged in both total energy and charge to errors of the order 10^{-5} . We have also minimized the total energy with respect to the lattice constant. The quoted results are those for the minimum configuration. No short ranged order due to chemical clustering has been taken into account in these calculations, nor any lattice distortions due to the size differences between the two constituents.

The estimates of the Curie temperature were obtained from the magnetic pair energies [13] The pair energies are defined as follows : At two sites labelled \underline{r} and \underline{r}' in a completely random paramagnetic background, we replace the potential by that of either the up-spin ferromagnetic Ni or the down-spin one. The Green function of this system we shall denote by : $G_{LL}^{Ni,\sigma\sigma'}(\underline{r},\underline{r},E)$, σ being the spin type at the site \underline{r} (either \uparrow or \downarrow) and σ' that at the site \underline{r}' . The pair energy is defined as

$$E(\underline{R}) = \int_{-\infty}^{E_F} dE E \left[-(1/\pi) \Im m \left(G_{LL}^{Ni,\uparrow\uparrow}(\underline{r},\underline{r},E) + G_{LL}^{Ni,\downarrow\downarrow}(\underline{r},\underline{r},E) \dots \right. \right. \\ \left. \left. - G_{LL}^{Ni,\uparrow\downarrow}(\underline{r},\underline{r},E) - G_{LL}^{Ni,\downarrow\uparrow}(\underline{r},\underline{r},E) \right) \right]$$

Here $\underline{R} = \underline{r} - \underline{r}'$. We may either estimate the above directly, or to be more accurate we may use the orbital peeling method of Burke [14]. The latter is an extension of the recursion method, where small differences of large energies (as in the definition of the pair energy) are obtained directly and accurately from the recursion continued fraction coefficients. Note that we have assumed that the dominant contribution to the pair energy comes from the band contribution and the rest approximately cancel out. The simplest Bragg-Williams estimate of the Curie temperature is

$$T_c = (1 - x)E(\underline{Q})/\kappa_B$$

where

$E(\underline{Q}) = E(\underline{q} = \underline{Q})$ and $E(\underline{q}) = \sum_{\underline{R}} \exp(i\underline{q} \cdot \underline{R}) E(\underline{R})$. Since the pair energy is short-ranged, a reasonable estimate of $E(\underline{Q})$ is $\sum_{n < 3} Z_n E(\underline{R}_n)$ where \underline{R}_n is the n^{th} -nearest

neighbour vectors and Z_n is the number of n^{th} -nearest neighbours. The Bragg-Williams approach overestimates the Curie temperature and its generalization, the cluster variation method, yields better quantitative estimates. We have restricted ourselves to the Bragg-Williams, nearest neighbour pair energy approximation.

3. Results and Discussion

In the phase diagram for NiMo alloys we notice first that the solid solution phase occupies a small part of the phase diagram below $x=0.12$ and extends down upto the lowest temperatures. In this region there is no transition to an ordered phase at low temperatures. This is the concentration region that we have focussed on in this communication.

Figure 1 shows the partial density of states for Ni and Mo. The full curves show the majority spin partial density of states and the dashed curves those for the minority spin. The Mo atomic concentrations are (i) 2% (ii) 4% (iii) 10% and (iv) 14%. The exchange splitting of the Ni d -states decrease with increasing Mo concentration. Exchange effects on Mo is very small and there is a very small induced moment on Mo atoms at low concentrations. Since we are interested in the shape of the density of states, the figure shows them in arbitrary units scaled between 0 and 1. The Fermi energies lie in the region just above -0.2 ryd.

Figure 2 shows the local magnetic moment in bohr-magneton/atom as a function of the Mo concentration. The short dashed curve are CPA results, while the long dashed curve shows the results from the ASR. In the low concentration regime, the CPA consistently gives larger magnetic moments. To compare with experiment, we convert the magnetic moment to magnetization in units of kA/m. The ASR results are shown in figure 3. The experimental data of Khan *et al* [5] are shown as squares. We first note that the ASR results for the very low Mo concentration regime agree rather well with experiment, while the CPA results are consistently higher. Khan *et al* suggest that the magnetization vanishes around concentration of 8% of Mo. The rigid band model predict a transition around 10%, while both the CPA and the ASR predict a transition around 12 to 13% of Mo. How do we reconcile these discrepancies? The rigid band model does not take into account charge transfer due to alloying between Ni and Mo, so cannot be quantitatively accurate. Our theoretical results actually calculate the magnetization per atom in a ferromagnetic arrangement. Here the local and global magnetizations are the same. The experimental results yield the average global magnetization $m = (1/N) \sum m_{loc}$. NiMo like all typical spin-glass alloys, is a solid solution of a magnetic constituent Ni and a non-magnetic one, Mo. Therefore, like all spin-glass alloys, we expect a paramagnetic-spin-glass transition around the concentration region 8%-13% of Mo. The experimental global magnetization

experiments will show a vanishing magnetization, whereas, our calculations will not show this. More detailed experiments like Mossbauer, low -field dc-susceptibility, hysteresis and so on, need to be done in this concentration region to get a better picture. This regime promises richness and variety in magnetic behaviour.

Figure 4 plots the Curie temperature versus concentration of Mo. Qualitatively the behaviour is in agreement with the results of Khan *et al.* The Bragg-Williams approximation used here is known to consistently overestimate the transition temperature. These results also indicate absence of transition from paramagnetic to an ordered phase at around 12% of Mo. Again, this is not surprising in the context of the discussion above. Our theoretical model also does not incorporate the possibility of a spin-disordered phase which becomes energetically favourable at around 8% Mo concentration.

We conclude with the remark that the concentration regime 8%-14% Mo requires both more careful experimental studies as well as more elaborate theoretical models which incorporate the possibility of the spin-disordered phase as well.

Acknowledgements

ND would like to thank the CSIR, India for financial assistance. AM acknowledges useful discussions with Dr. G.P. Das and Prof. A.K. Majumdar.

References

- [1] *Binary Alloy Phase Diagrams* ed. T.B. Massalski(ASM International) 1990
- [2] Das G P, Salunke H and Banerjee S 1997 *Bull. Mat. Sci.* **20** 787
- [3] Andersen O K and Jepsen O 1984 *Phys. Rev. Lett.* **53** 2571
- [4] Saha T, Dasgupta I and Mookerjee A 1994 *J. Phys.: Condens. Matter* **6** L245 (1994)
- [5] Khan F A, Asgar M A and Nordblad P 1997 *J. Magn. Magn. Mater.* **174** 121
- [6] Andersen O K, Jepsen O and Krier H 1991 *Electronic Structure of Metals and Alloys* ed. Andersen O K, Kumar V and Mookerjee A (World Scientific)
- [7] Dasgupta I, Saha T and Mookerjee A 1996 *J. Phys.: Condens. Matter* **8** 1979
- [8] Mookerjee A and Prasad R 1985 *Phys. Rev.* **B48**; Dasgupta I, Saha T and Mookerjee A 1993 *Phys. Rev.* **B51** 17724
- [9] Saha T, Dasgupta I and Mookerjee A 1995 *J. Phys.: Condens. Matter* 3413
- [10] Luchini M U and Nex C M M 1987 *J. Phys. C: Solid State Phys.* **20** 3125
- [11] Ghosh S, Das N and Mookerjee A 1997 *J. Phys.: Condens. Matter* **9** 10701
- [12] Ghosh S, Das N and Mookerjee A 1998 *Int.J.Mod.Phys.* 1998 B (submitted)
- [13] Mookerjee A 1998 *Electron correlations in atoms and solids* ed. Tripathi A N and Singh I (Phoenix Publishing House, New Delhi) pp 180-198
- [14] Burke N E 1976 *Surf.Sci.* **58** 349

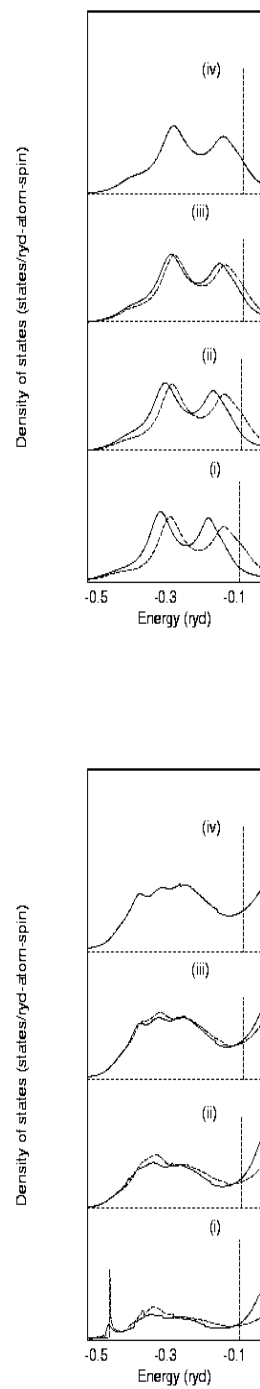


Figure 1. The partial densities of states of Ni and Mo at 2,6,10 and 14 atomic % of Mo. Dashed curves show the results for the minority and full curve the majority spin states.

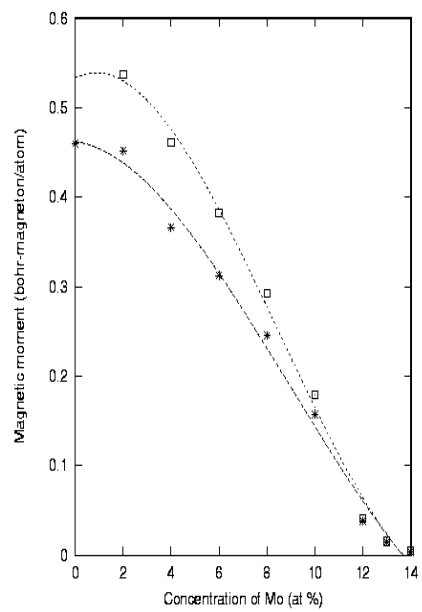


Figure 2. The magnetic moment on Ni as a function of Mo concentration. Stars refer to the augmented space calculations while the squares to the CPA.

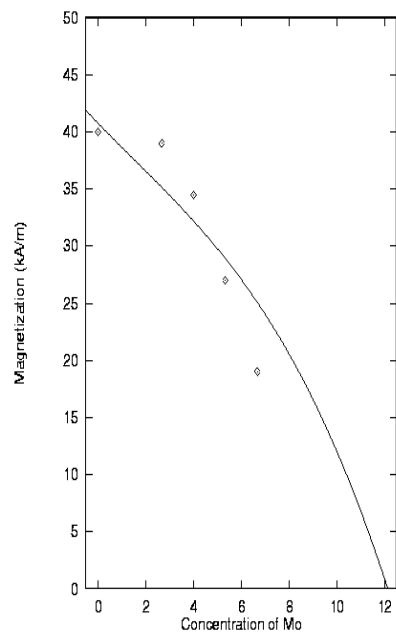


Figure 3. The magnetization as a function of Mo concentration at 0K obtained from the theoretical estimates.

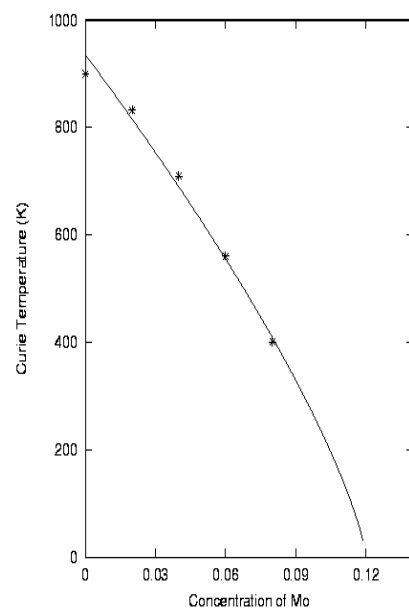


Figure 4. The Curie temperature as a function of Mo concentration.